
Oday I. ABDULLAH*, **Wassan Abd AL-SAHB****,
Abdullah M. Al-SHABIBI***

THERMOELASTIC ANALYSIS OF MULTI-DISC CLUTCHES USING FINITE ELEMENT METHOD

ANALIZA TERMOSPREŻYSTA SPRZĘGŁA WIELOTARCZOWEGO ZA POMOCĄ METODY ELEMENTU SKOŃCZONEGO

Key words:

dry friction, Multi-disc clutch, FEM, thermoelastic behaviour, temperature field

Słowa kluczowe:

tarcie suche, sprzęgło wielotarczowe, MES, zachowanie termosprężyste, pole temperatury

Summary:

The high thermal stresses generated between the contacting surfaces of a multi-disc clutch system (pressure plate, clutch discs, plate separators, and piston) due to the frictional heating generated during slipping are considered to be one

* Department of System Technologies and Mechanical Design Methodology Hamburg University of Technology, Germany, e-mail: oday.abdullah@tu-harburg.de.

** Department of Mechanical Eng. / College of Eng. / University of Baghdad, Iraq.

*** Department of Mechanical and Industrial Eng. / College of Eng. / Sultan Qaboos University, Oman.

of the main reasons for clutch failure related to contact surfaces. A finite element technique has been used to study the transient thermoelastic phenomena of a multi-disc dry clutch. The results present the contact pressure distribution, the temperature evaluation, and the heat flux generated along the frictional surfaces. Analysis has been completed using two-dimensional axisymmetric model to simulate the multi-disc clutch. ANSYS software has been used to perform the numerical calculation in this paper.

INTRODUCTION

Automotive clutches and brakes are frequently subjected to high thermal loads, and this load will occur as a result of slipping between contact surfaces. The surface temperatures may cause serious disadvantages, such as thermal cracks and permanent deformation, and these conditions will lead to premature failure of the sliding systems in some cases.

Al-Shabibi and Barber [L. 1] investigated an alternative method to solve the thermoelastic contact problem with frictional heat generation. A two-dimensional axisymmetric finite element model was built to study the temperature field and pressure distribution of two sliding disks. Constant and varying speeds were considered in this analysis. The results show that the initial temperature is shown to be crucial, since it represents the particular solution, which can have quite an irregular form, and this situation especially true when the system operates above the critical speed.

Ivanović et al. [L. 2] presented a pragmatic semi-physical approach to modelling the thermal dynamic behaviour of a wet clutch. The thermal energy balance was considered the base to investigate the heat transfer mechanisms in the separator plate. The coefficient of friction behaviour and thermal dynamics are considered the most important parameters that effect on the wet clutch dynamics response. Moreover, the effect of the coefficient of friction on the clutch slip speed, the applied force, and friction surface temperatures have been studied. The results of the dynamic thermal model were experimentally validated.

Zagrodzki [L. 3] studied the frictional heating in the sliding systems and the effect of sliding speed on the stability of the system when the sliding speed exceeds the critical value. The finite element model used to investigate the transient thermo-elastic process, spatial discretization and modal superposition is presented. Constant sliding speed was performed in this analysis. The transient salutation includes both the homogenous part (corresponding to the initial condition) and the non-homogenous part (represent the background process). The results show that the important parameters that are contributors in the background process are the nominal process equivalent to uniform pressure distribution in isothermal case and the pressure variation caused by geometric imperfection or by design features.

Jang and Khonsari [L. 4] presented a newly developed model to predicting the rate of the growth of instability in a conductor-insulator system in the presence of a liquid lubricant and found a relation between the wave speed and the configurations of hot spots. The analysis includes terms for the roughness of the surface and is capable of treating bodies of finite thickness with or without lubrication. The results show that the shape of hot spots is more likely to be circular with an appreciable penetration depth when the wave speed is small, and the hot spots is elongated when the wave speed is much slower than the operating speed.

Zhang et al. [L. 5] developed a new model for wet clutches in hydrodynamic machineries to compute the thermal behaviour with high accuracy. Matlab/Simulink was used to build the model and find the temperature field during engagement. The shift schedule, piston pressure, and relative velocity parameters were considered in this Simulink model. A two-dimensional heat conduction model was used to calculate the temperature distribution along the axial direction and radial direction on the sliding interface between contact surfaces. The results have shown a good agreement with the experimental work.

Seo et al. [L. 6] suggested a thermal model to estimate the temperature distribution for a wet clutch in 4WD coupling to avoid thermal failure for the clutch plate during operating conditions of vehicle. The results of this model are validated experimentally with an actual 4WD vehicle under a limitation of a torque = 900 Nm. The theoretical results have shown a good agreement with the experimental results.

Czél et al [L. 7] used a finite element method for a dry ceramic clutch disk to find the thermal behaviour and compared it with experimental measurement results. The heat partition factor and heat convection coefficient were assumed to be changing in time and space. A distributed heat source was applied for modelling heat generation. The thermal results have shown a good agreement with the measured temperature.

Abdullah and Schlattmann [L. 8–12] investigated the temperature field and the energy dissipated of a dry friction clutch during a single and repeated engagement under uniform pressure and uniform wear conditions. They also studied the effect of pressure between contact surfaces when varying with time on the temperature field and the internal energy of clutch disc using two approaches. One was the heat partition ratio approach to compute the heat generated for each part individually, and the second applies the total heat generated for the whole model using a contact model. Furthermore, they studied the effect of engagement time and sliding velocity function, thermal load, and dimensionless disc radius (inner disc radius/outer disc radius) on the thermal behaviour of the friction clutch in the beginning of engagement.

This paper presents full details to compute the temperature field and contact pressure distribution of multi-disc dry friction clutch during the beginning of engagement. The finite element method used to obtain the numerical simulation of the transient thermo elastic properties of the clutch system. The pressure applied during the period of engagement was assumed constant and the effect of convection is neglected.

FUNDAMENTAL PRINCIPLES

The main system of the multi-disc dry friction clutches consists of a pressure plate, clutch discs, plate separators, and a piston as shown in **Fig. 1**. When the clutch starts to engage, slipping will occur between contact surfaces due to the difference in the velocities between them (slipping period), after this period, all contacts parts are rotating at the same velocity without slipping (full engagement period). A high amount of the kinetic energy is converted into heat energy at interfaces, according to the first law of thermodynamics, during the slipping period; and the heat generated between contact surfaces will be dissipated by conduction between friction clutch components and by convection to the environment, and in addition to the thermal effect due to the slipping, there is other load condition which is the pressure contact between contact surfaces. In the second period, there are three types of load conditions: the temperature distribution from the last period (slipping period), the pressure between contact surfaces due to the axial force, and the centrifugal force due to the rotation of the contacts parts. **Figure 2** shows the load conditions during the engagement cycle of the clutch system, where t_s is the slipping time and T is the transmitted torque by clutch.

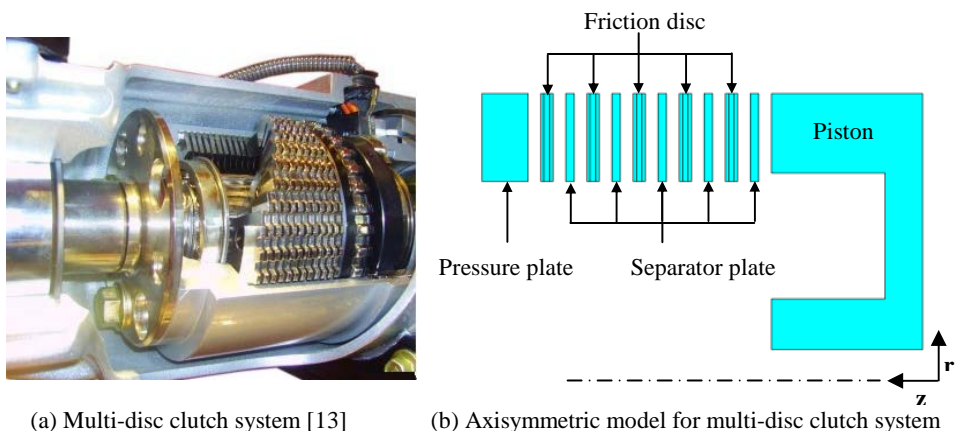


Fig. 1. The main parts of a Multi-disc clutch

Rys.1. Główne komponenty sprzęgła wielotarczowego: system sprzęgła wielotarczowego, b) model osiowosymetryczny sprzęgła wielotarczowego

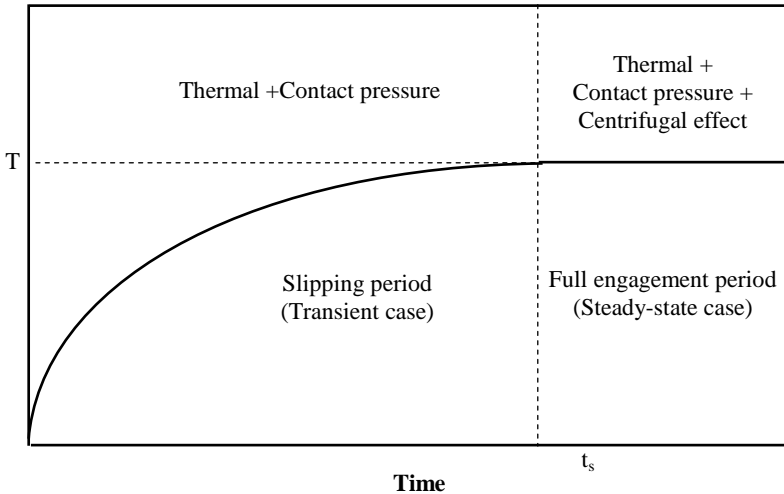


Fig. 2. The load conditions during the engagement cycle of the clutch

Rys. 2. Warunki obciążenia podczas cyklu pracy sprzęgła

FINITE ELEMENT FORMULATION

This section presents the steps to simulate the contact elements of a friction clutch using ANSYS software. Moreover, it gives more details about the types of contacts and algorithms that are used in this software.

The first step in this analysis is the modelling. Due to the symmetry in the geometry (frictional lining without grooves) and boundary conditions of the friction clutch (take into the consideration the effect of the pressure and the thermal load due to the slipping), a two-dimensional axisymmetric FEM can be used to represent the contact between the clutch elements during the slipping period. The axisymmetric model of the multi-disc clutch system with boundary conditions is shown in **Fig. 3 (a)**, and the effect of convection is neglected in this analysis.

There are three basic types of contact used in ANSYS software are single contact, node-to-surface contact, and surface-to-surface contact. Surface-to-surface contact is the most common type of contact used for bodies that have arbitrary shapes with relative large contact areas. This type of contact is most efficient for bodies that experience large values of relative sliding, such as block sliding or plane or sphere sliding within a groove [L. 14]. Surface-to-surface contact is the type of contact assumed in this analysis because of the large areas of clutch elements in contact.

The elements used for contact elastic model are as follows:

- “Plan13” used for all elements of the clutch system (piston, clutch discs, separator plates, and pressure plate);

- “Conta172” used for contact surfaces that are the both surfaces of clutch discs; and,
- “Targe169” used for the target surfaces that are the surfaces of the separator plates and the surface of the pressure plate that contact with the friction disc.

The element used for the heat conduction model is Plane55. **Figure 3 (b)** shows the finite element model of multi-clutch disc that has been used in this analysis.

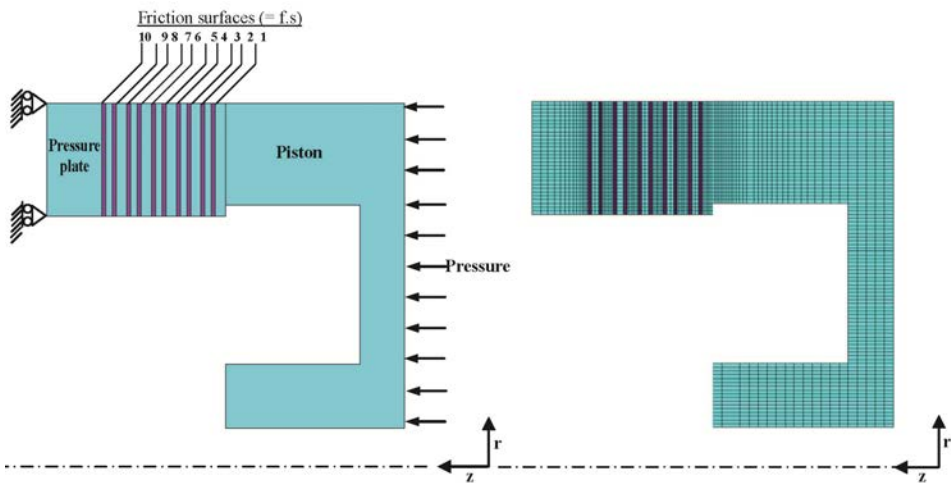


Fig. 3a. The Contact model with boundary conditions of multi-disc clutch system

Rys. 3a. Model styku z warunkami brzegowymi

Fig. 3b. FE model of multi-disc clutch system (No. of elements= 4428)

Rys. 3b. Model MES sprzęgła wielotarczowego (liczba elementów 4428)

There are five algorithms used for surface-to-surface contact type as follows:

- Penalty method: This algorithm used constant “spring” to establish the relationship between the two contact surfaces (**Figure 4**). The contact force (pressure) between two contact bodies can be written as follows:

$$F_n = k_n x_p \quad (1)$$

Where, F_n is the contact force, k_n is the contact stiffness, and x_p is the distance between two existing nodes or separate contact bodies (penetration or gap).

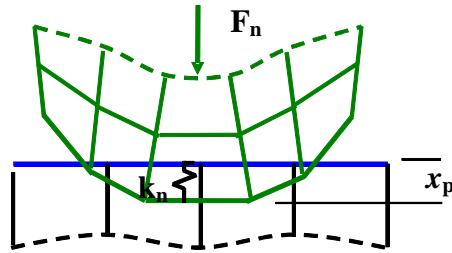


Fig. 4. The contact stiffness between two contact bodies

Rys. 4. Sztywność stykowa dwu kontaktujących się elementów

- Augmented Lagrange (default): This algorithm is an iterative penalty method. The constant traction (pressure and frictional stresses) are augmented during equilibrium iterations so that the final penetration is smaller than the allowable tolerance. This method usually leads to better conditioning and is less sensitive to the magnitude of the constant stiffness. The contact force (pressure) between two contact bodies is

$$F_n = k_n x_p + \lambda \quad (2)$$

Where, λ is the Lagrange multiplier component.

- Lagrange multiplier on contact for normal and penalty for tangent: This method is applied on the constant normal and penalty method (tangential contact stiffness) on the frictional plane. This method enforces zero penetration and allows a small amount of slip for the sticking contact condition. It requires chattering control parameters, as well as the maximum allowable elastic slip parameter.
- Pure Lagrange multiplier on contact for both normal and tangent: This method enforces zero penetration when contact is closed and “zero slip” when sticking contact occurs. This algorithm does not require contact stiffness. Instead, it requires chattering control parameters. This method adds contact traction to the model as additional degrees of freedom and requires additional iterations to stabilize contact conditions. It often increases the computational cost compared to the augmented Lagrangian method.
- Internal multipoint constraint: This method is used in conjunction with bonded contact and no separation contact to model several types of contact assemblies and kinematic constraints.

The Pure Lagrange multiplier method is the method used in this analysis to obtain the contact distribution between the contact surfaces of the clutch system.

A mesh sensitivity study was done to choose the optimum mesh from the computational accuracy point of view. The full Newton-Raphson with unsymmetrical matrices of elements is used in this analysis assuming a large-deflection effect. In all computations for the friction clutch model, it has been assumed a homogeneous and isotropic material, and all parameters and materials properties are listed in **Table. 1**. This analysis also assumed that there are no cracks in the contact surfaces.

In the numerical modelling of contact problems, special attention is required because the actual contact area between the contacting bodies is usually not known beforehand. In contact problems, unlike other boundary problems, nodes on the contact surface do not have prescribed displacements or tractions. Instead, they must satisfy two relationships: (1) the continuity of normal displacements on the contact surface (no overlap condition of contact area), and (2) the equilibrium conditions (equal and opposite tractions). Even if the contacting bodies are linear materials, contact problems are nonlinear because the contact area does not change linearly with the applied load. Accordingly, iterative or increment schemes are needed to obtain accurate solutions of contact problems. The iterations to obtain the actual contact surface are finished when all of these conditions are met [L. 15].

Figure 5 shows the interfaces of two adjacent subregions (i and j) of elastic bodies. The elastic contact problem is treated as quasi-static with standard unilateral contact conditions at the interfaces. The following constraint conditions of displacements are imposed on each interface:

$$w_i = w_j, \quad \text{if } P > 0 \quad (3)$$

$$w_i \leq w_j, \quad \text{if } P = 0 \quad (4)$$

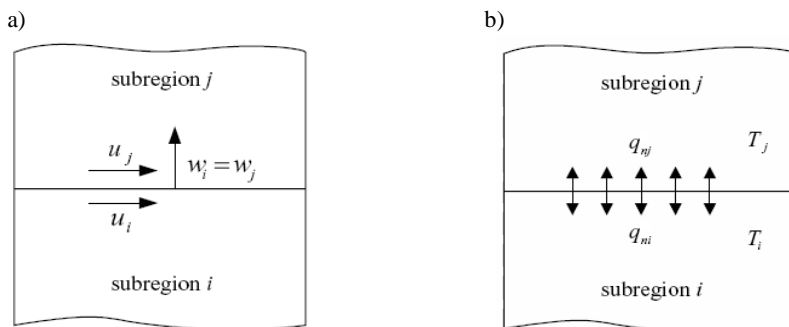


Fig. 5. Contact model for the (a) elastic and (b) heat conduction problem in two adjacent subregions

Rys. 5. Model styku dla problemu sprężystego (a) przewodzenia ciepła w dwu przylegających podobszarach

Where, P is the normal pressure on the friction surfaces. The radial component of the sliding velocity resulting from the deformations is considerably smaller than the circumferential component. Therefore, the frictional forces in the radial direction on the friction surfaces are disregarded in this study [L. 16]. **Figure 5 (b)** shows the thermal phenomena of two adjacent subregions of bodies. The interfacial thermal boundary conditions depend on the state of mechanical contact. Two unknown terms, q_{ni} and q_{nj} , exist on each interface. To fully define the heat transfer problem, two additional conditions are required on each contact interface. If the surfaces are in contact, the temperature continuity condition and the heat balance condition are imposed on each interface as follows:

$$T_i = T_j, \quad \text{if } P > 0 \quad (5)$$

$$q = \mu P \omega r = -\sum q_n = -(q_{ni} + q_{nj}), \quad \text{if } P > 0 \quad (6)$$

Where, μ and ω are the coefficients of friction and angular sliding velocity, respectively. Then, using the aforementioned conditions, equations of one node from each pair of contact nodes are removed. If the surfaces are not in contact, the separated surfaces are treated as an adiabatic condition:

$$q = 0 = q_{ni} = q_{nj}, \quad \text{if } P = 0 \quad (7)$$

Assume the sliding angular velocity decreases linearly with time as

$$\omega(t) = \omega_o \left(1 - \frac{t}{t_s}\right), \quad 0 \leq t \leq t_s \quad (8)$$

The distribution of the normal pressure P in Eq. (6) can be obtained by solving the mechanical problem occurring in the disc clutch.

Clutch engagement can be simulated through a direct computer simulation. The simulation involves solving two coupled problems at the same time. Given the temperature field $T(r, z, t)$, the thermoelastic contact problem is solved for the contact pressure $p(r, t)$. This is done by solving Hook's law with thermal strain relations

$$\varepsilon_{ij} = \frac{(1+\nu)}{E} \sigma_{ij} - \left(\frac{\nu}{E} \sigma_{mm} + \alpha T \right) \delta_{ij} \quad (9)$$

and equilibrium equations

$$\frac{\partial \sigma_{ij}}{\partial x_j} = 0 \quad (10)$$

and boundary conditions (3-5) that involve exposed surfaces and displacement constraints. The contact pressure from the thermoelastic problem is then used to define the frictional heat flux (6). The second problem that needs to be solved is the transient heat conduction equation,

$$\nabla^2 T = \frac{1}{k} \frac{\partial T}{\partial t} \quad (11)$$

to yield a new temperature field $T(r, z, t + \delta t)$. The boundary conditions of this problem involve the heat flux $q(r)$ given at the contact interface and some other boundaries, which can consist of convective and insulated surfaces.

Table 1. The properties of materials and operations

Tabela 1. Własności materiałów i warunki pracy

Parameters	Values
Inner radius of friction clutch disc, r_i [m]	0.052
Outer radius of friction clutch disc, r_o [m]	0.067
Thickness of clutch disc including the friction surfaces [m], t_t	0.00193
Thickness of the friction material [m], t_{fr}	0.00053
Inner radius of pressure plate [m], r_{ip}	0.052
Outer radius of pressure plate [m], r_{op}	0.067
Thickness of the pressure plate [m], t_p	0.0074
Inner radiuses of piston [m], r_{if1} and r_{if2}	0.0235 0.0535
Outer radiuses of piston [m], r_{of1} and r_{of2}	0.032 0.067
Thicknesses of the piston [m], t_{f1} and t_{f2}	0.006 0.024
pressure, p [MPa]	1
Coefficient of friction, μ	0.2
Number of friction clutch disc, n	5
Maximum angular slipping speed, ω_o [rad/sec]	300
Young's modulus for friction material, E_{fr} [GPa]	0.30
Young's modulus for pressure plate, plate separator, piston & clutch plate, (E_p , E_f and E_{cp}), [Gpa]	125
Poisson's ratio for friction material,	0.25
Poisson's ratio for pressure plate, plate separator, piston & clutch plate	0.25
Density for friction material, [kg/m^3], ρ_{fr}	2000
Density for pressure plate, plate separator, piston & clutch plate, [kg/m^3], (ρ_p , ρ_f and ρ_{cp})	7800
Specific heat for friction material, [J/kg K]	120
Specific heat for pressure plate, plate separator, piston & clutch plate, [J/kg K]	532
Conductivity for friction material, [W/mK]	1
Conductivity for pressure plate, plate separator, piston & clutch plate, K_p , K_f & , K_{cp} [W/mK]	54
Thermal expansion for friction material and steel [K^{-1}]	$12e^{-6}$
Slipping time, t_s [s]	0.5

A schematic diagram representing the finite element simulation is shown in **Fig. 6**. The simulation involves constructing two different models. The first of which is used to solve the thermoelastic problem to yield displacement field and contact pressure distribution. The other model is used to solve the transient heat conduction problem to account for the change in the temperature field. The two models are coupled through the fact that the contact pressure from the first model is needed in the second model to define the frictional heat flux. Moreover, the temperature field from the heat conduction model is needed for the computation of the contact pressure. This requires defining short time steps during which the contact pressure and the sliding speed are assumed to remain constant.

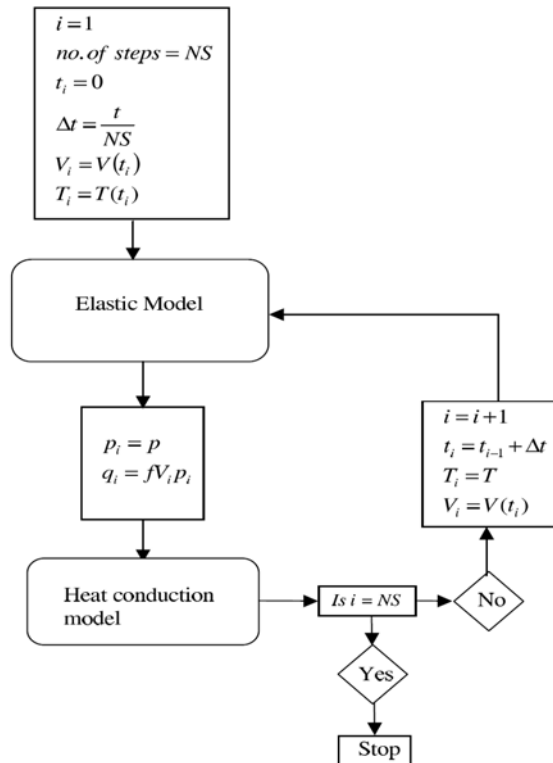


Fig. 6. Schematic diagram of FE simulation [L. 1]

Rys. 6. Schematyczny diagram symulacji MES

RESULTS AND DISCUSSIONS

The numerical model is simulated using the finite element method to investigate the thermoelastic behaviour of multi-disc clutch system. The simulation consists of two models. The first is the elastic contact model that is

used to calculate the pressure distribution between contact surfaces. The second is the heat conduction model used to calculate the temperature field of the multi-disc clutch with time.

Figures (7–16) show the pressure distribution on the friction surfaces ($f \cdot s = 1$ to 10) at different time (0.2 s, 0.4 s, 0.6 s, 0.8 s and 1 s). At the initial of engagement, the pressure distribution on each friction surface is almost uniform, except the first and the last surfaces are not uniform distributed, and the reason for these results is that the thermoelastic effects are small until this time. However, after time passes, at time 0.2 s, the trend of the normal pressure distribution on each friction surface obviously shows the thermoelastic effects. In general, the distribution of pressures on friction surfaces can undergo changes due to the thermal deformations, which is known as the thermoelastic transition. This process of the growth of non-uniformity in the pressure distribution can be unstable, and then the TEI phenomenon takes place in the sliding system. The maximum and minimum values of contact pressure occur at the end of the slipping period in the last friction surface ($f \cdot s = 10$) and the 4th friction surface ($f \cdot s = 4$), respectively.

Figure 17 show the variation of the heat flux with disc radius for different friction surfaces ($f \cdot s = 1, 3, 5, 7$ & 9) at $t = 0.4$ s. It can be seen that the maximum values of heat flux occur at the last friction surface.

The variation of the maximum temperature with time is shown in **Figure 18**. The temperature increases from the initial temperatures 0K to maximum temperature 602.4K at $t = 0.4$ s and then the temperature decreases to the final temperature 572.3K at the end of the slipping $t = 0.5$ s.

Figures (19–21) show the contour of the temperature distribution of the multi-disc clutch system. It can be seen that the values of temperature grow from a minimum value at $t = 0$ to a maximum value at $t = 0.8$ s. The temperature on each friction surface increases due to the increment of normal pressure as a whole, and especially, the temperature profiles on friction surface 10 partially change due to the localized rise in normal pressures.

CONCLUSIONS

In this paper, the solution of the transient homogeneous thermoelastic analysis of multi-disc clutch system during the beginning of engagement (slipping period) has been performed. A two dimensional axisymmetric finite element model was built to obtain the contact pressure distribution and temperature field of the multi-disc clutch system. It can be seen that the higher values of contact pressure occur at the last friction disc ($f \cdot s = 9$ & 10), and this situation will lead to a high generation of heat in these contact surfaces and consequently the maximum values of temperatures occur at these surfaces. The effect of the thermoplastic phenomena starts on the clutch system at $t = 0.1$ s.

The maximum values of temperature occur in the last friction disc at $t \approx 0.4$ s (0.8ts) during the slipping period of 0.5 s. The maximum values of contact pressure occur near the mean radius at $t = 0.5$ s for all friction discs ($f \cdot s = 1$ to 8) except the last one occurs ($f \cdot s = 9$ & 10) at $t = 0.4$ s. This study presents a valuable design tool to investigating the effect of thermoelastic phenomena on the multi-disc clutch system behaviour during the beginning of engagement.

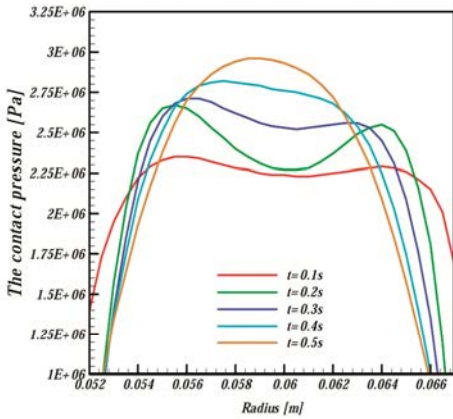


Fig. 7. Contact pressure distribution on the 1st friction surface at selected time intervals

Rys. 7. Rozkład nacisków stykowych na 1. powierzchni tarcia

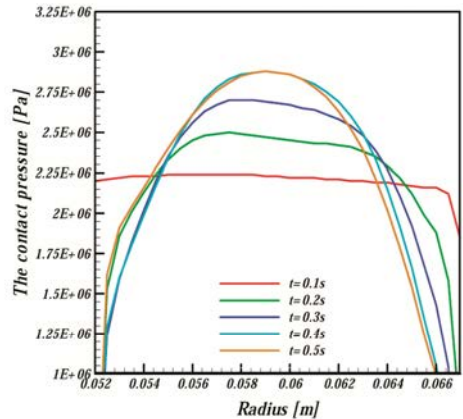


Fig. 8. Contact pressure distribution on the 2nd friction surface at selected time intervals

Rys. 8. Rozkład nacisków stykowych na 2. powierzchni tarcia

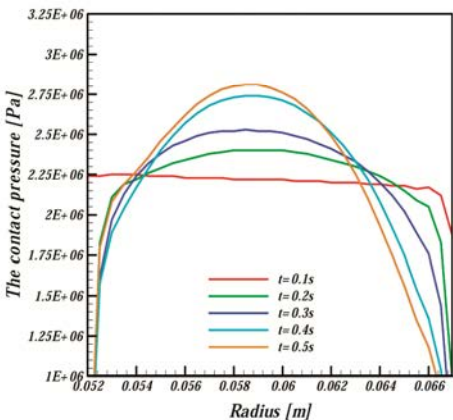


Fig. 9. Contact pressure distribution on the 3rd friction surface at selected time intervals

Rys. 9. Rozkład nacisków stykowych na 3. powierzchni tarcia

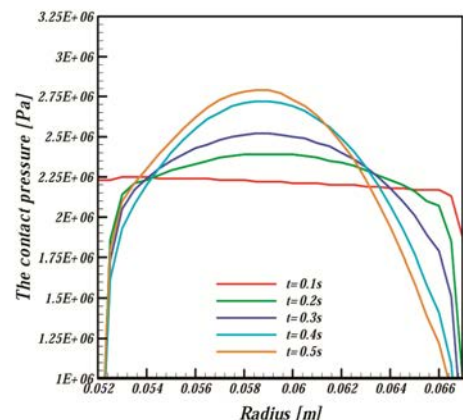


Fig. 10. Contact pressure distribution on the 4th friction surface at selected time intervals

Rys. 10. Rozkład nacisków stykowych na 4. powierzchni tarcia

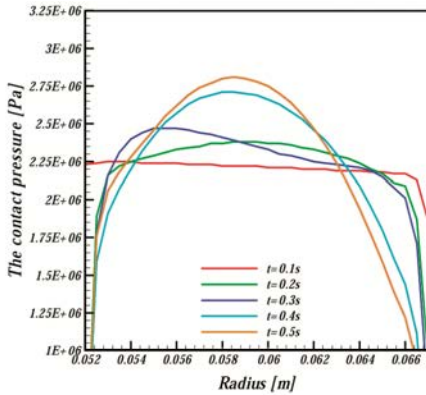


Fig. 11. Contact pressure distribution on the 5th friction surface at selected time intervals

Rys. 11. Rozkład nacisków stykowych na 5. powierzchni tarcia

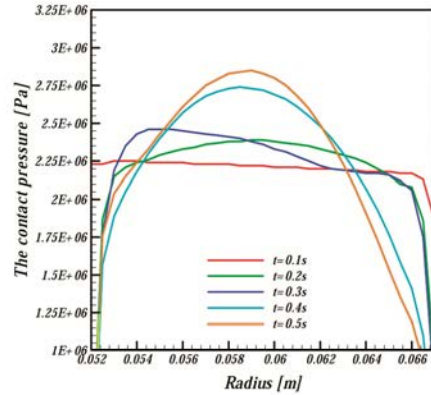


Fig. 12. Contact pressure distribution on the 6th friction surface at selected time intervals

Rys. 12. Rozkład nacisków stykowych na 6. powierzchni tarcia

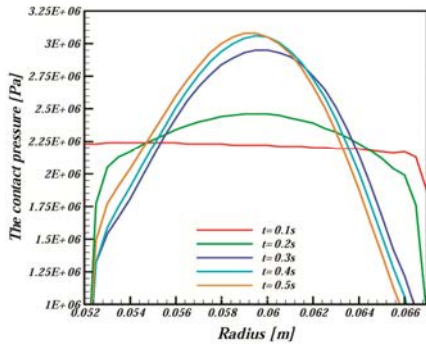


Fig. 13. Contact pressure distribution on the 7th friction surface at selected time intervals

Rys. 13. Rozkład nacisków stykowych na 7. powierzchni tarcia

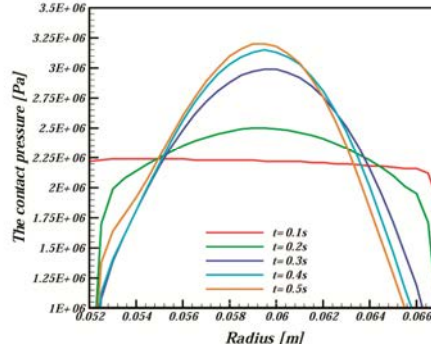


Fig. 14. Contact pressure distribution on the 8th friction surface at selected time intervals

Rys. 14. Rozkład nacisków stykowych na 8. powierzchni tarcia

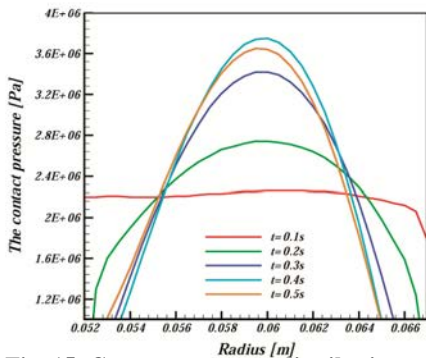


Fig. 15. Contact pressure distribution on the 9th friction surface at selected time intervals

Rys. 15. Rozkład nacisków stykowych na 9. powierzchni tarcia

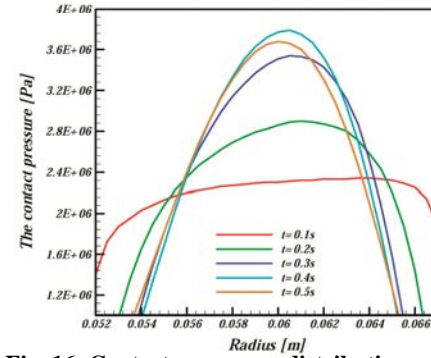


Fig. 16. Contact pressure distribution on the 10th friction surface at selected time intervals

Rys. 16. Rozkład nacisków stykowych na 10. powierzchni tarcia

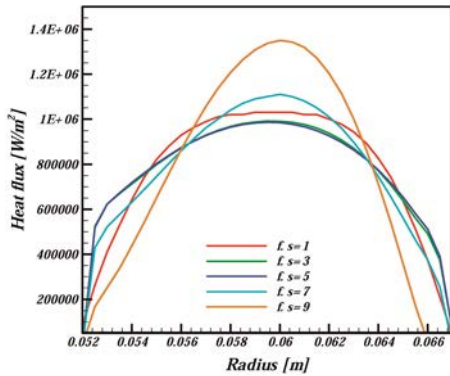


Fig. 17. Variation of heat flux with disc radius for selected friction surfaces at $t=0.4$ s

Rys. 17. Zmienność strumienia ciepła w funkcji promienia dla $t = 0,4$ s

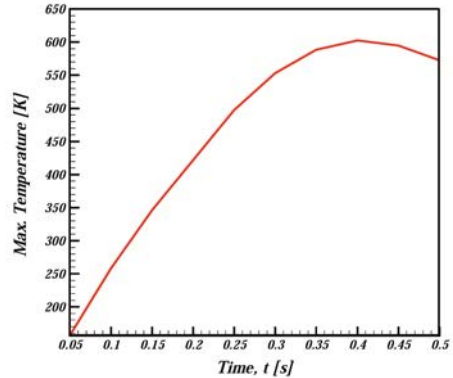


Fig. 18. The maximum temperature history of the multi-disc clutch system

Rys. 18. Przebieg czasowy temperatury maksymalnej dla sprzęgła wielotarczowego

REFERENCES

1. Al-Shabibi A.M., Barber J.R.: "Transient Solution of the Unperturbed Thermoelastic Contact Problem", *Journal of Thermal Stresses* Vol. 32, Issue 3, 2009, pp. 226–243.
2. Ivanović V., Herold Z., Deur J.: "Experimental Characterization of Wet Clutch Friction Behaviors Including Thermal Dynamics", *SAE International Journal of Engines* 2009 vol. 2 no. 1, pp. 1211–1220.
3. Zagrodzki P.: "Thermoelastic instability in friction clutches and brakes- Transient modal analysis revealing mechanisms of excitation of unstable modes", *Int. J. of Solids and Structures*, Vol. 46, 2009, pp. 2463–2476.
4. Jang J.Y., Khonsari M.M.: "On the Growth Rate of Thermoelastic Instability", *Transactions of the ASME*, Vol. 126, 2004, pp. 50–55.
5. Jin-Le Zhang, Biao Ma, Ying-Feng Zhang and He-Yan Li: "Simulation and Experimental Studies on the Temperature Field of a Wet Shift Clutch during one Engagement", *Int. Conf. of Computational Intelligence and Software Eng. (CiSE) 2009 IEEE*, 2009.
6. Howon Seo, Chunhua Zheng, Wonsik Lim, Suk Won Cha, Sangchull Han: "The results have shown a good agreement with the experimental work", *Vehicle Power and Propulsion Conference (VPPC)*, 2011 IEEE.
7. Czél B., Váradi K., Albers A., Mitariu M.: 'Fe thermal analysis of a ceramic clutch', *Tribology International* 45, pp. 714–723 (2009).
8. Oday I.A., Schlattmann J.: The Effect of Disc Radius on Heat Flux and Temperature Distribution in Friction Clutches, *J. Advanced Materials Research*, Vol. 505, pp. 154–164, 2012.
9. Abdullah O.I., Schlattmann J.: Finite Element Analysis of Dry Friction Clutch with Radial and Circumferential Grooves, *Proceeding of World Academy of Science, Engineering and Technology Conference*, Paris, pp. 1279–1291, 2012.

10. Abdullah O.I., Schlattmann J.: Effect of Band Contact on the Temperature Distribution for Dry Friction Clutch, Proceeding of World Academy of Science, Engineering and Technology Conference, Berlin, pp. 167–177, 2012.
11. Oday I.A., Schlattmann J.: The Correction Factor for Rate of Energy Generated in the Friction Clutches under Uniform Pressure Condition, J. Adv. Theor. Appl. Mech., Vol. 5, no. 6, pp. 277–290, 2012.
12. Abdullah O.I., Schlattmann J.: Finite Element Analysis of Temperature Field in Automotive Dry Friction Clutch, J. Tribology in Industry, Vol. 34, No. 4, pp. 206–216, 2012.
13. ANSYS Contact Technology Guide, ANSYS Release 11.0 Documentation, ANSYS, Inc.
14. <http://www.kfz-tech.de>.
15. Becker A.A.: The Boundary Element Method in Engineering, McGraw-Hill, New York, 1992.
16. Zagrodzki P.: Analysis of thermomechanical phenomena in multi-disc clutches and brakes, Wear 140 (1990) 291–308.

Streszczenie

Wysokie naprężenia cieplne generowane między stykającymi się powierzchniami systemu sprzęgła wielotarczowego (tarcza dociskowa stała, tarcze sprzęgłowe, tarcze rozdzielające, tarcza dociskowa ruchoma) w wyniku tarcia ślizgowego są uważane za jedną z głównych przyczyn uszkodzeń powierzchni stykowych sprzęgła. Do badania nieustalonych przebiegów termosprężystych w suchym sprzęgle wielotarczowym zastosowano metodę elementu skończonego (MES). Wyniki przedstawiają rozkład nacisków stykowych, ocenę temperatury i strumienia ciepła generowanego na powierzchniach ciernych. Analizę przeprowadzono z zastosowaniem dwuwymiarowego modelu osiowoosymetrycznego symulującego sprzęgło wielotarczowe. Użyto oprogramowania ANSYS do przeprowadzenia obliczeń numerycznych w niniejszej pracy.